Protein Structures

DOI: 10.1002/ange.201210015

Probing the Conformational Diversity of Cancer-Associated Mutations in p53 with Ion-Mobility Mass Spectrometry**

*Ewa Jurneczko, Faye Cruickshank, Massimiliano Porrini, David J. Clarke, Iain D. G. Campuzano, Michael Morris, Penka V. Nikolova, and Perdita E. Barran**

The tumor suppressor p53 is the most mutated protein in human cancers. It is implicated in lung (70%), colon (60%), and stomach (45%) cancers, respectively.[1] The latest release (R16) of the International Agency for Research on Cancer (IARC) TP53 mutation database contains 29575 somatic mutations (November 2012; http://www-p53.iarc.fr/). A distinctive feature of the p53 mutational map is the rate of occurrence of missense mutations. Indeed, these single-point amino acid substitutions in p53 lead to abrogation of protein function, rather than deletions or nonsense mutations, as it is the case with most tumour suppressor proteins. A technique that is able to rapidly distinguish p53 mutants at low concentrations could have marked benefits for cancer screening assays and also for drug discovery. In this study, we used ion-mobility mass spectrometry (IM-MS) for this task.

The p53 protein contains 393 amino acids and is divided into several structural and functional domains (Figure 1a): a transactivation domain (TAD, residues 1–61, a proline-rich fragment (PR, residues 62–94) with multiple copies of the PXXP sequence, a DNA- binding domain (DBD, residues 94–292), a tetramerization domain (TET, residues 325–355), and a strongly basic C-terminal regulatory domain (CT, residues 363–393).[2] Very few mutations have been reported in the N- or C-terminal domains.[3] The central core of the protein, consisting of the DNA-binding domain, is the most highly conserved domain and is required for sequence-specific DNA binding. The majority of tumour-derived mutations (over 95%) are mapped to the DBD, where the cluster of six so-called "hot spots" is located.[4] The structure of the p53 DBD was first solved by Cho et al. in 1994.[5] Based on the structure,

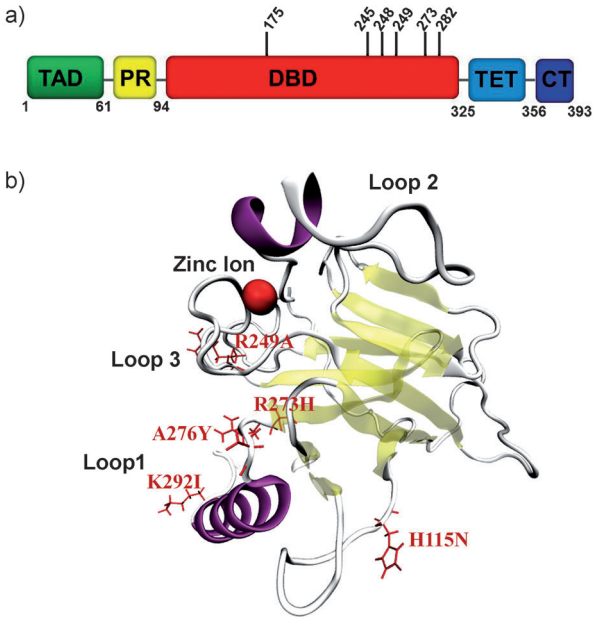

Figure 1. Structure of protein p53. a) Domain structure of full-length p53 with six highlighted mutational "hot spots". b) Structure of human p53 DBD. Locations of residues mutated in the experiments described herein are labeled in red, the zinc atom is represented as a red sphere (PDB: 2FEJ; image generated using the VMD software).

the "hot spots" were classified as "structural" or "contact" mutations. These residues can affect either the thermodynamic stability and hence the structural integrity of the p53 DBD, or the conformation of the protein required for protein–DNA or protein–protein interactions.[2,6–11]

Herein, we report IM-MS studies on the conformational diversity of wild-type p53 and common cancer-associated p53 mutants. We define "conformational phenotypes" and monitor the variation in these as exhibited by four single-point mutations: R249A, R273H, K292I, and A276Y. Locations of mutated residues used in the studies are depicted schematically on the 3D structure of p53 (Figure 1b). Specifically, we test whether the second-site suppressor mutant from loop L1, H115N, could trigger conformational changes in p53 cancer-associated mutations. In addition we use mass spectrometry as a tool to test the DNA-binding properties of the wild-type (WT) p53 and H115N mutant proteins.

IM-MS can provide detailed insights into the structures of macromolecular systems.[12–16] Measured drift times are recorded as arrival-time distributions (ATDs), which can then be converted into collision cross sections (CCSs).[17,18] In this study, a Synapt HDMS[19] (Waters Corporation, Man-

[*] E. Jurneczko, F. Cruickshank, Dr. M. Porrini, Dr. D. J. Clarke, Dr. P. E. Barran
The EastChem School of Chemistry, The University of Edinburgh
West Mains Road, EH9 3JJ, Edinburgh (UK)
E-mail: perdita.barran@ed.ac.uk
Dr. P. V. Nikolova
School of Biomedical Science, Institute of Pharmaceutical Sciences, King's College London
150 Stamford Street, SE1 9NH, London (UK)
Dr. I. D. G. Campuzano,[+] Dr. M. Morris
Waters MS Technology Centre, Micromass Atlas Park
Simonsway, M22 5PP, Manchester (UK)
[+] Present address: Department of Molecular Structure, Amgen Inc. One Amgen Center Drive, Thousand Oaks, CA 91320 (USA)

[**] This work has been funded by the award of a BBSRC Strategic Industrial Case studentship to E.J. in collaboration with Waters MS technologies.

Supporting information for this article is available on the WWW under http://dx.doi.org/10.1002/anie.201210015.

chester, UK) and in-house-modified drift-tube (DT) IM-MS were used.[20]

In the absence of DNA and under near-neutral conditions, the WT p53 DBD exists mainly as a zinc-bound monomer (calculated $M_R = 24615.5$ Da, observed $M_R = 24612.4$ Da) with the two major signals corresponding to $[M+9H]^{9+}$ and $[M+10H]^{10+}$ (Figure S1 A). This narrow spread of charge states is usually indicative of a compact protein with a low number of residues available for protonation in solution. Higher-charged species ($11 \le z \le 18$) are present with significantly lower abundance, thus providing evidence for a small population of more unfolded states of p53 in solution. IM-MS analysis quantitates the conformational flexibility of p53 in vacuo implied by the charge-state distribution (Figure 2 a). The majority of the protein molecules in the charge states $z = 9^+$ and 10^+ are indeed compact conformers (C1), which also exist when $z = 11^+$, 12^+, and 13^+, although the signal intensity is reduced with each additional charge state and the conformation of the protein molecules shifts to a more extended form called X1. For $11 \le z \le 18$, multiple unfoldomers (Un) are observed in each charge state, and the number of resolvable Un conformers is at least four, albeit at low intensity. The lack of baseline resolution in the arrival-time distributions suggests interconverting conformers for these extended forms. Using the trajectory method approach established by Jarrold and co-workers,[21,22] we calculated

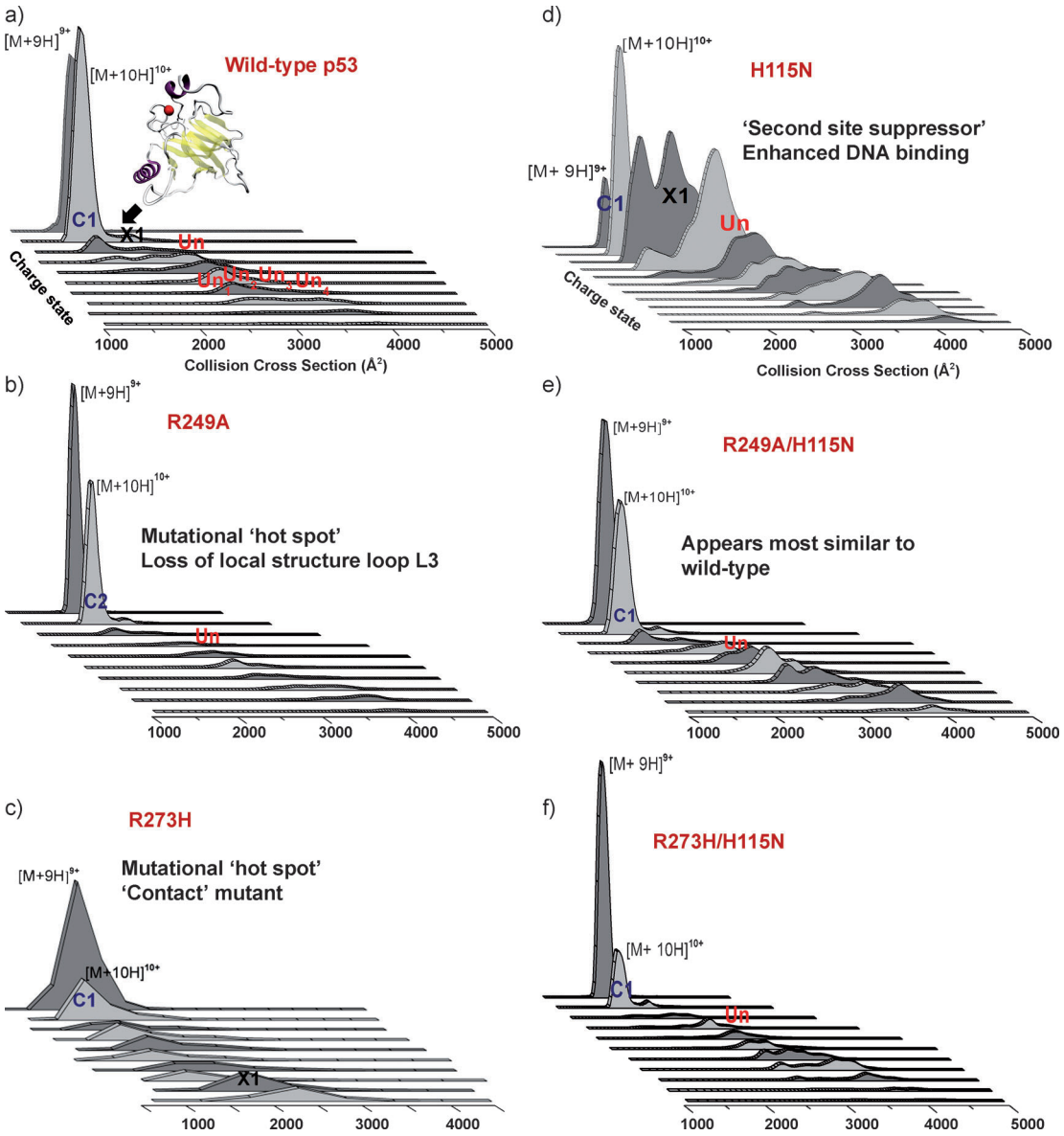

Figure 2. Waterfall plots representing the in vacuo "conformational phenotypes" of the p53 DBD sprayed from buffered conditions (50 mM ammonium acetate, containing 10 vol% propan-2-ol). The *x*, *y*, and *z* axis show the collision cross section (CCS, in Å^2), charge state (range: $9 \le z \le 18$), and the relative intensity, respectively. The plots show the abundance of the conformations present within the protein, here a range of extended conformers for the higher charge states is observed. a) Wild-type p53, b) R249A, c) R273H, d) H115N, e) R249A/H115N, f) R273H/H115N. All data were obtained on the TW IM-MS with the exception of the R273H mutant, which was acquired on the drift-tube IM-MS instrument (the data shown here were recorded at a 60 V electric potential across the drift cell).

the CCS from coordinates obtained from the X-ray crystal structure of p53 deposited by Wang et al. (PDB: 2OCJ),[23] and found a CSS of 2072 Å^2. The lowest experimentally observable charge states have a smaller CCS than those calculated using MOBCAL, thus indicating that the protein has collapsed somewhat in comparison to the X-ray structure (supporting the general tendency we have previously reported for monomeric proteins[12]). The CCS value of the second, much less populated family of conformers, which starts with the more extended conformer (X1) for $z = 10^+$ (2157 Å^2), coincides with the CCS value calculated from crystal structure coordinates (Figure 2a), but more extended forms are also present, suggesting unfoldomers (U_n).

One of the most common mutational 'hot spots' is at position arginine 249, which is replaced by serine, thus causing the loss of the local structure in loop L3 and distorting the remainder of the DNA-binding surface.[9,24] Here we examined the related mutation R249A with IM-MS (Figure 2b; see the Supporting Information, Figure S1B for the mass spectrum). When compared to WT p53, it is clear that this single-point mutation inflicts a dramatic change to the conformational space occupied by the protein, with the R249A mutant possessing noticeably less flexibility. The majority of R249A presents as $z = 9^+$ and 10^+ ions, both in a compact form with similar CCSs (1789 Å^2 and 1818 Å^2, respectively) as for the C1 form of the WT p53, although the width of the ATDs for the mutant is less than that for the WT, thus implying a more "molten globule-like" compact conformer for this single-point mutant, which we here denote C2. The 9^+ charge state is also more intense here compared to WT p53, which suggests a more compact structure. For $11 \le z \le 18$, multiple unfoldomers (Un) for each charge state are observed. However these extended conformers are less populated than in WT p53. Overall, the gas-phase structure of R249A favors a compact geometry, suggesting that the mutation conferred intrinsic stability to a collapsed form, which is significantly smaller (by 14%) than that found in WT p53.

The second class of cancer-associated mutants, such as R273H, are present at the p53 DNA-binding interface and referred to as "DNA contact" mutants, representing about 20% of all mutants in the p53 database.[4,7] They have marginal effect on the stability, but affect the conformation required for DNA binding.[9] Introduction of the imidazole ring by the histidine residue has been reported to perturb the local environment, and to break a salt bridge between R273 and the carboxylate group of D281 in helix 2.[25] Data for this mutation were obtained using DT IM-MS (Figure 2c; see the Supporting Information Figure S1C for the mass spectrum). Here the compact conformation is retained over a large range of charge states ($9 \le z \le 16$) and the more extended forms (X1) are only present at the very high charge states. This remarkable stability of a compact conformation and the lack of unfoldomers indicate that this mutation favors more compact and rigid conformations.

Cellular levels of p53 are controlled elaborately through ubiquitylation and proteasomal degradation, which are mediated by numerous E3 ubiquitin ligases. Interestingly, there are two sequentially located lysine residues in the p53 DBD, K291, and K292, which are required for polyubiquitination and degradation of p53 mediated by makorin ring finger protein 1 (MKRN1).[26] These two highly conserved residues are mutated in several different types of human tumors, suggesting their critical roles in p53 function.[3] We examined the "conformational phenotype" exhibited by one of these cancer-associated mutants, K292I, which is implicated in the inhibition of protein–protein interactions (see the Supporting Information, Figure S2A; Figure S1D for the mass spectrum). Here a single compact conformation is only exhibited by $z = 10^+$ (C2), gradually shifting to more extended structures (X1). For $10 \le z \le 18$, multiple unfoldomers are observed and their distribution is comparable to that of the WT p53. Another mutation, A276Y, is an example of a 'contact' mutation as it directly binds to DNA.[5,27] However, the substitution of the alanine residue with a larger aromatic amino acid also has a significant effect on the function of the protein. This mutation maps to the binding sites of protein kinases and Mdm2, a major regulator of p53 levels in the cell.[28] In mobility space (see the Supporting Information, Figure S2B; Figure S1H for the mass spectrum) the majority of the protein molecules are located in the $z = 9^+$ and 10^+ region, and exist as a compact conformer (C2). Remarkably, this compact form of the protein is retained over a wide range of charge states ($9 \le z \le 14$) and its signal intensity is significantly higher than that of all previously shown mutants or WT p53 proteins. For $10 \le z \le 18$, multiple unfoldomers (Un) are observed. The intensity of the latter is spread over a very broad distribution of conformers; for instance for $z = 17^+$, at least four unfoldomers can be resolved, centered at 2778 Å^2, 3049 Å^2, 3689 Å^2, and 4046 Å^2. An extraordinary feature of this substitution is that both compact forms and more extended conformations are highly populated and stable over a longer mobility time, which is in marked contrast with other mutants or WT p53 proteins.

Based on the vital role of p53 in carcinogenesis, it is not surprising that the identification of strategies to restore function to cancer-associated mutants has attracted great interest. Engineered mutation H115N in the loop L1 (known as a mutational "cold spot") of the DBD has been exploited as a "second-site suppressor" in a double mutation approach that aims to restore function to cancer-associated p53 mutants.[24] This mutant protein possesses superior DNA-binding properties and is thermally more stable than WT p53.[24,29] When we performed IM-MS analysis to provide a conformational "finger print" of H115N (Figure 2d), we observed a broader distribution of conformers relative to the WT p53. According to our mass spectrometry results (Figure S1E), the protein has a similar range of charge states ($9 \le z \le 19$) as the WT p53 protein, however the higher charge states present with higher intensity. In IM-MS, the conformational diversity of this engineered mutant is remarkable. For $z = 9^+$ and 10^+, a C1-type conformer with a CCS averaging 1730 Å^2 is observed, but for $z = 11^+$, the intensity is spread over a wide distribution of conformers from C1, with a CCS of 1827 Å^2, to X1 with a CCS centered on 2184 Å^2. From mass spectrometry space (see the Supporting Information, Figure S1E for the mass spectrum) we know that the intensity of the more extended populations is more pronounced, but IM-MS provides another dimension to this analysis, thus indicat-

ing that this mutant is intrinsically more plastic and significantly more disordered than the WT p53.

Figure 2e shows IM-MS data for the double mutant R249A/H115N (see the Supporting Information, Figure S1F for the mass spectrum). Here the effect of the "second site suppressor" H115N becomes more apparent. In mobility space, the conformational occupancy of this double mutant appears highly similar to that presented by WT p53. The highly abundant low charge states show an increased width in their ATDs, which is indicative of a C1 conformer as opposed to the more narrow C2 conformer, but remarkably the extended conformers Un are noticeably more populated than in the WT p53. It appears that the double mutant presents a juxtaposition of the conformational space presented by each single mutant, providing not just a visual reference but more critically details on the conformational spread afforded by the double mutant. This method has important implications for drug discovery. For example, a small-molecule inhibitor that might mimic the function of the H115N mutation could be screened by using this IM-MS approach. Finally we consider the impact of H115N as a "second-site suppressor" on the contact mutant R273H (Figure 2f; see the Supporting Information, Figure S1G for the mass spectrum). Again the conformational signature of the double mutant is highly comparable to that of the WT p53 and the plasticity of the H115N mutant has increased the population of the more extended forms of the protein. The data in Figure 2a–c shows the power of IM-MS in showing the effects of a single oncogenic mutation on p53 DBD on the fraction of folded and unfolded protein. In the following section, we use IM-MS to probe the DNA-binding ability of the p53 DBD. In order to do this, we used a 12-mer double-stranded DNA (containing two consensus binding sites) to probe the binding capacity of the WT p53 and H115N mutant proteins. p53 is known to regulate the gene transcription by binding to over 100 different, naturally occurring DNA-binding sites or response elements.[19] The isolated p53 DBD binds specifically to double-stranded DNA sequence of two tandem decameric elements PuPuPuC(A/T)(A/T)GPyPyPy (Pu = A/G,Py = T/C) that can be separated by 0–13 base pairs.[31] In the absence of DNA, the p53 DBD exists mainly as a free monomer in solution and is also capable of weak monomer–monomer interactions (see the Supporting Information, Figure S1A). In the presence of DNA, we find that p53 possesses a remarkable self-organizing ability (Figure 3). The WT p53 DBD consistently binds consensus double-stranded DNA as a 2:1 complex only ($z = 12^+$–15^+; Figure 3a). In mobility space, the 2:1 p53 DBD/DNA complex exists only as a single conformation, with CCS values only minimally higher (mass corrected) compared to the dimeric form without DNA (for instance, for the $z = 14^+$ complex, a CCS of 3196 Å^2 was measured, and for the $z = 14^+$ dimer, a CCS of 2644 Å^2 was measured), thus suggesting a tight association of this complex. In case of the H115N mutation, we only observe a 2:1 protein/DNA complex, thus implicating that the binding is strongly cooperative. The data supports the superior DNA-binding ability of this mutant. The p53 H115N DBD/DNA complex is much more pronounced and has a wider charge-state distribution ($z = 12^+$–18^+; Figure 3b). The stoichiometric

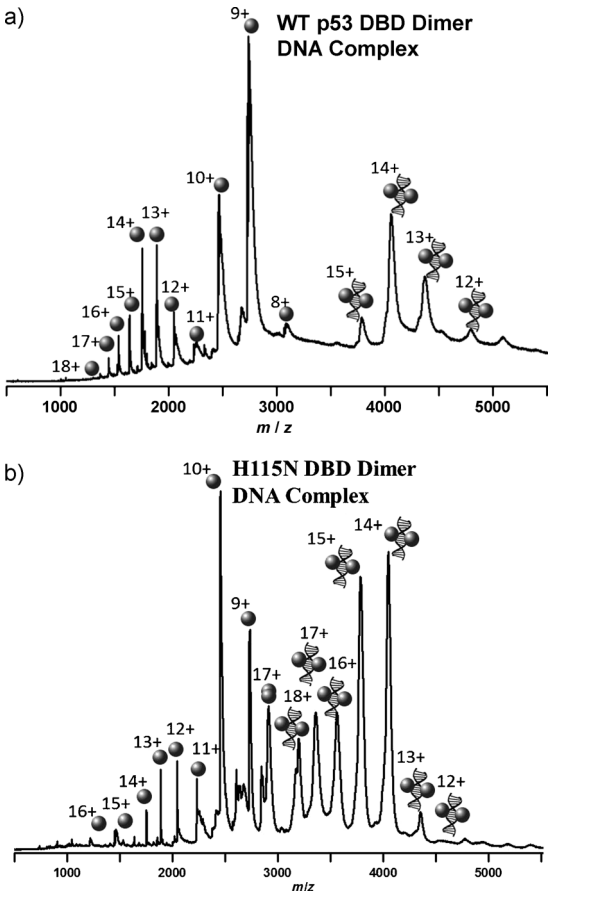

Figure 3. ESI mass spectra of the p53 DBD with a double-stranded 12-base-pair DNA fragment. a) Wild-type p53 DBD with a double-stranded 12-base-pair DNA in a ratio of 2:1 (protein to DNA, based on a protein monomer). b) H115N mutant with a double-stranded 12-base-pair DNA in a ratio of 7:1 (protein to DNA, based on a protein monomer). Both spectra were obtained from a solution buffered with ammonium acetate, and recorded on the DT IM-MS. The single spheres on the left represents a p53 monomer, whereas the spheres with DNA spirals correspond to the dimeric p53/DNA complex.

amount of DNA to the protein had to be radically decreased (Figure S3) in order to remove the excess of unbound DNA present in the mass spectrum, thus providing clear evidence of improved DNA-binding activities for this mutation. IM-MS data for this mutation show that the 2:1 H115N DBD/DNA complex favors a single conformational state. The CCSs are centered around similar values as the corresponding charge states of the 2:1 WT p53 complex. Since the p53 DBD evidently associates only when binding to consensus DNA, it is possible that it undergoes allosteric conformational changes as it forms a dimeric complex. Evidence for allosteric regulation of DNA binding in wild-type p53 is already available.[32–36] Interestingly, the oligomerization clearly chaperoned by DNA is possible without the tetramerization domain.

We have demonstrated the application of IM-MS and its capabilities for probing the conformation flexibility of p53 carcinogenic mutants. This novel application of IM-MS could be exploited in elucidation of the relationship between p53 antineoplastic activities and its structure and functions, as well

as in other medically important proteins in the human genome. The striking ability of this technique to delineate the stoichiometry and the conformational spread of this tumor suppressor protein in the presence of binding partners will provide unparalleled insights to its structure–function relationships.

Experimental Section

Protein purification and expression is described in the Supporting Information. The buffers of all protein samples were exchanged with 50 mM ammonium acetate using Slide-A-Lyzer dialysis cassettes (Fisher Scientific, UK). Mass spectrometry and mobility data were acquired either on Synapt HDMS[19] (Waters Corporation, Manchester, UK) or on in-house-modified drift-tube (DT) IM-MS.[20] The instrumental conditions are detailed in the Supporting Information.

Received: December 14, 2012
Published online: March 14, 2013

Keywords: conformation analysis · DNA · mass spectrometry · p53 protein · protein structures

[1] L. Bai, W.-G. Zhu, *J. Cancer Mol.* **2006**, *2*, 141 – 153.
[2] A. C. Joerger, A. R. Fersht, *Annu. Rev. Biochem.* **2008**, *77*, 557 – 582.
[3] http://www-p53.iarc.fr/.
[4] J. Xu, J. Reumers, J. R. Couceiro, F. De Smet, R. Gallardo, S. Rudyak, A. Cornelis, J. Rozenski, A. Zwolinska, J.-C. Marine, D. Lambrechts, Y.-A. Suh, F. Rousseau, J. Schymkowitz, *Nat. Chem. Biol.* **2011**, *7*, 285 – 295.
[5] Y. Cho, S. Gorina, P. D. Jeffrey, N. P. Pavletich, *Science* **1994**, *265*, 346 – 355.
[6] A. C. Joerger, A. R. Fersht, F. V. W. a. G. K. George, *Adv. Cancer Res.* **2007**, *97*, 1 – 23.
[7] A. N. Bullock, J. Henckel, B. S. DeDecker, C. M. Johnson, P. V. Nikolova, M. R. Proctor, D. P. Lane, A. R. Fersht, *Proc. Natl. Acad. Sci. USA* **1997**, *94*, 14338 – 14342.
[8] P. V. Nikolova, K.-B. Wong, B. DeDecker, J. Henckel, A. R. Fersht, *EMBO J.* **2000**, *19*, 370 – 378.
[9] H. C. Ang, A. C. Joerger, S. Mayer, A. R. Fersht, *J. Biol. Chem.* **2006**, *281*, 21934 – 21941.
[10] Y. Pan, B. Ma, R. B. Venkataraghavan, A. J. Levine, R. Nussinov, *Biochemistry* **2005**, *44*, 1423 – 1432.
[11] Y. Pan, R. Nussinov, *J. Phys. Chem. B* **2008**, *112*, 6716 – 6724.
[12] E. Jurneczko, P. E. Barran, *Analyst* **2011**, *136*, 20 – 28.
[13] C. Uetrecht, R. J. Rose, E. van Duijn, K. Lorenzen, A. J. R. Heck, *Chem. Soc. Rev.* **2010**, *39*, 1633 – 1655.
[14] B. C. Bohrer, S. I. Merenbloom, S. L. Koeniger, A. E. Hilderbrand, D. E. Clemmer, *Annu. Rev. Anal. Chem.* **2008**, *1*, 293 – 327.
[15] B. T. Ruotolo, J. L. P. Benesch, A. M. Sandercock, S.-J. Hyung, C. V. Robinson, *Nat. Protoc.* **2008**, *3*, 1139 – 1152.
[16] E. Jurneczko, M. Porrini, P. Nikolova, I. D. Campuzano, M. Morris, P. E. Barran, *Biochem. Soc. Trans.* **2012**, *40*, 1021 – 1026.
[17] M. F. Bush, Z. Hall, K. Giles, J. Hoyes, C. V. Robinson, B. T. Ruotolo, *Anal. Chem.* **2010**, *82*, 9557 – 9565.
[18] E. A. Mason, E. W. McDaniel, *Transport Properties of Ions in Gases*, John Wiley & Sons, Inc., New York, **1988**, pp. 1 – 29.
[19] S. D. Pringle, K. Giles, J. L. Wildgoose, J. P. Williams, S. E. Slade, K. Thalassinos, R. H. Bateman, M. T. Bowers, J. H. Scrivens, *Int. J. Mass Spectrom.* **2007**, *261*, 1 – 12.
[20] B. J. McCullough, J. Kalapothakis, H. Eastwood, P. Kemper, D. MacMillan, K. Taylor, J. Dorin, P. E. Barran, *Anal. Chem.* **2008**, *80*, 6336 – 6344.
[21] A. A. Shvartsburg, M. F. Jarrold, *Chem. Phys. Lett.* **1996**, *261*, 86 – 91.
[22] M. F. Mesleh, J. M. Hunter, A. A. Shvartsburg, G. C. Schatz, M. F. Jarrold, *J. Phys. Chem.* **1996**, *100*, 16082 – 16086.
[23] Y. Wang, A. Rosengarth, H. Luecke, *Acta Crystallogr. Sect. D* **2007**, *63*, 276 – 281.
[24] A. Merabet, H. Houlleberghs, K. Maclagan, E. Akanho, T. T. Bui, B. Pagano, A. F. Drake, F. Fraternali, P. V. Nikolova, *Biochem. J.* **2010**, *427*, 225 – 236.
[25] K. B. Wong, B. S. DeDecker, S. M. Freund, M. R. Proctor, M. Bycroft, A. R. Fersht, *Proc. Natl. Acad. Sci. USA* **1999**, *96*, 8438 – 8442.
[26] E.-W. Lee, M.-S. Lee, S. Camus, J. Ghim, M.-R. Yang, W. Oh, N.-C. Ha, D. P. Lane, J. Song, *EMBO J.* **2009**, *28*, 2100 – 2113.
[27] M. Kitayner, H. Rozenberg, N. Kessler, D. Rabinovich, L. Shaulov, T. E. Haran, Z. Shakked, *Mol. Cell* **2006**, *22*, 741 – 753.
[28] M. H. G. Kubbutat, S. N. Jones, K. H. Vousden, *Nature* **1997**, *387*, 299 – 303.
[29] J. Ahn, M. V. Poyurovsky, N. Baptiste, R. Beckerman, C. Cain, M. Mattia, K. McKinney, J. Zhou, A. Zupnick, V. Gottifredi, C. Prives, *Cell Cycle* **2009**, *8*, 1603 – 1615.
[30] T. Tokino, S. Thiagalingam, W. S. el-Deiry, T. Waldman, K. W. Kinzler, B. Vogelstein, *Hum. Mol. Genet.* **1994**, *3*, 1537 – 1542.
[31] S. E. Kern, K. W. Kinzler, A. Bruskin, D. Jarosz, P. Friedman, C. Prives, B. Vogelstein, *Science* **1991**, *252*, 1708 – 1711.
[32] J. L. Waterman, J. L. Shenk, T. D. Halazonetis, *EMBO J.* **1995**, *14*, 512 – 519.
[33] T. D. Halazonetis, L. J. Davis, A. N. Kandil, *EMBO J.* **1993**, *12*, 1021 – 1028.
[34] T. D. Halazonetis, A. N. Kandil, *EMBO J.* **1993**, *12*, 5057 – 5064.
[35] J. E. Stenger, P. Tegtmeyer, G. A. Mayr, M. Reed, Y. Wang, P. Wang, P. V. Hough, I. A. Mastrangelo, *EMBO J.* **1994**, *13*, 6011 – 6020.
[36] P. Balagurumoorthy, H. Sakamoto, M. S. Lewis, N. Zambrano, G. M. Clore, A. M. Gronenborn, E. Appella, R. E. Harrington, *Proc. Natl. Acad. Sci. USA* **1995**, *92*, 8591 – 8595.

